Journal of Sound and Vibration (1990) **136**(1), 141–145

LETTERS TO THE EDITOR

MODAL ANALYSIS OF A HERMETIC CAN

1. INTRODUCTION

Recently we described the State Space Method (SSM), a transfer matrix based substructuring technique, and verified it through its successful application to various axisymmetric shell structures including a refrigeration compressor shell [1, 2]. Now in this communication we further demonstrate the applicability of SSM by considering a hermetic can which is composed of a circular cylinder with two circular end plates as shown in Figure 1. Analytical results are compared with model measurements, and some difficulties typically associated with the experiment are also identified.

2. FORMULATION

The state vector at any arbitrary location along the meridian of the structure shown in Figure 1 is $\{\Phi(x)\}^T = \langle W_1, W_2, W_3, \beta_x, M_x, N_x, V_x, S_{x\theta}\rangle$ (a list of nomenclature is given in the Appendix). The state vector at the mid-section A–A of the cylinder, $\{\Phi(x_{1c})\}$, is expressed in terms of the state vector at the initial boundary near the center of the end plate, $\{\Phi(x_{0p})\}$, by using the overall transfer matrix, $[T(x_{0p}, x_{1c})]$, according to

$$\{\Phi(x_{1c})\} = [T(x_{0p}, x_{1c})]\{\Phi(x_{0p})\}, \tag{1}$$

where $[T(x_{0p}, x_{1c})] = [T(x_{0c}, x_{1c})][C][T(x_{0p}, x_{1p})]$. Here, subscripts p and c denote plate and cylinder, respectively. The cylinder and the end plates are coupled through the coupling matrix $[C]$, the non-zero elements of which are $C_{22} = C_{31} = C_{44} = -C_{13} = 1$, and $C_{55} = C_{76} = C_{88} = -C_{67} = D_c/D_p$.

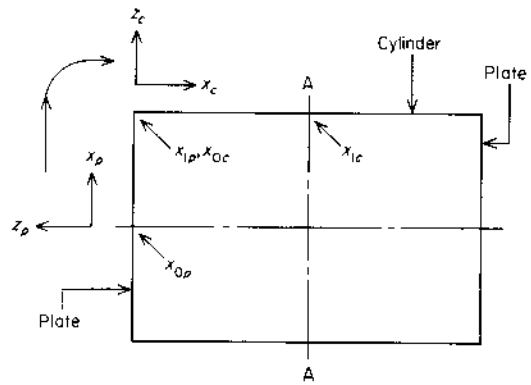

Figure 1. Cross-sectional view of the hermetic can.

Since SSM requires distinct boundaries, and since the eigenproblem becomes singular at the center of the end plate, a "pinhole" with free edges is introduced at the center of the end plate as the initial boundary. The ratio of the diameter of this pinhole to the

0022-460X/90/010141+05 $03.00/0

diameter of the end plate is 1%. This approximate modeling of the solid circular end plate has been shown to allow an accurate determination of the eigenvalues and eigenfunctions [3]; however, it may produce inaccurate moment and force estimations near the center of the plate.

The initial boundary condition enforced at the pinhole is $\{\Phi(x_{0p})\}^T = \langle W_1, W_2, W_3, \beta_x, 0, 0, 0, 0\rangle$. A similar condition could be applied at the pinhole of the second end plate as the final boundary condition. However, the computational effort is reduced if one takes advantage of the structural symmetry about the midsection A–A shown in Figure 1. Therefore, the final boundary condition enforced at the midsection A–A of the cylinder is $\{\Phi(x_{1c})\}^T = \langle W_1, 0, 0, \beta_x, 0, 0, V_x, S_{x\theta}\rangle$ for antisymmetric modes about A–A, and $\{\Phi(x_{1c})\}^T = \langle 0, W_2, W_3, 0, M_x, N_x, 0, 0\rangle$ for symmetric modes about A–A. Implementing these boundary conditions in equation (1), and partitioning the overall transfer matrix appropriately, one formulates the eigenproblem which is then solved numerically for the natural frequencies and modes shapes of the overall structure; see reference [1] for further details.

3. ANALYTICAL RESULTS

The procedure is applied to a hermetic can which is 228·6 mm in diameter, 347 mm in length, and 2 mm in thickness, and is made of steel with $E = 207$ GPa, $\rho = 7800$ kg/m^3, and $\nu = 0{\cdot}3$. The first three natural frequencies predicted by SSM for a given circumferential mode number n are listed in Table 1, along with results obtained by the Finite Element Method (FEM), using a commercial software with an axisymmetric conical shell element. As seen from Table 1, SSM and FEM results are in excellent agreement except for the $n = 1$ mode. For unknown reasons, this deviation occurs only for those $n = 1$ modes which are dominated by the motion of the end plates [1, 3]. Further investigation of this biased error is necessary. Various SSM mode shapes are shown in Figure 2. For the lower circumferential modes $n = 0$ and 1, the end plates seem to assume the role of the primary vibrating substrates with little participation of the cylinder. A larger degree of coupling

TABLE 1

Hermetic can: comparison of SSM *and* FEM *natural frequencies* (Hz)

	Symmetric modes			Antisymmetric modes		
n	SSM	FEM	Δ%	SSM	FEM	Δ%
0	359	359	0·0	388	388	0·0
	1412	1409	0·2	1452	1450	0·1
	3173	3166	0·2	3230	3222	0·2
1	783	746	4·7	788	752	4·6
	2218	2152	3·0	2221	2155	3·0
	3799	3802	−0·1	4201	4130	1·7
2	1210	1208	0·2	1226	1223	0·2
	1276	1276	0·0	2862	2859	0·1
	2991	2982	0·3	3122	3119	0·1
3	793	793	0·0	1787	1785	0·1
	1799	1797	0·1	2165	2166	0·0
	3414	3417	−0·1	3902	3896	0·2

$\Delta\% = 100 \times (\text{SSM} - \text{FEM})/\text{SSM}$.

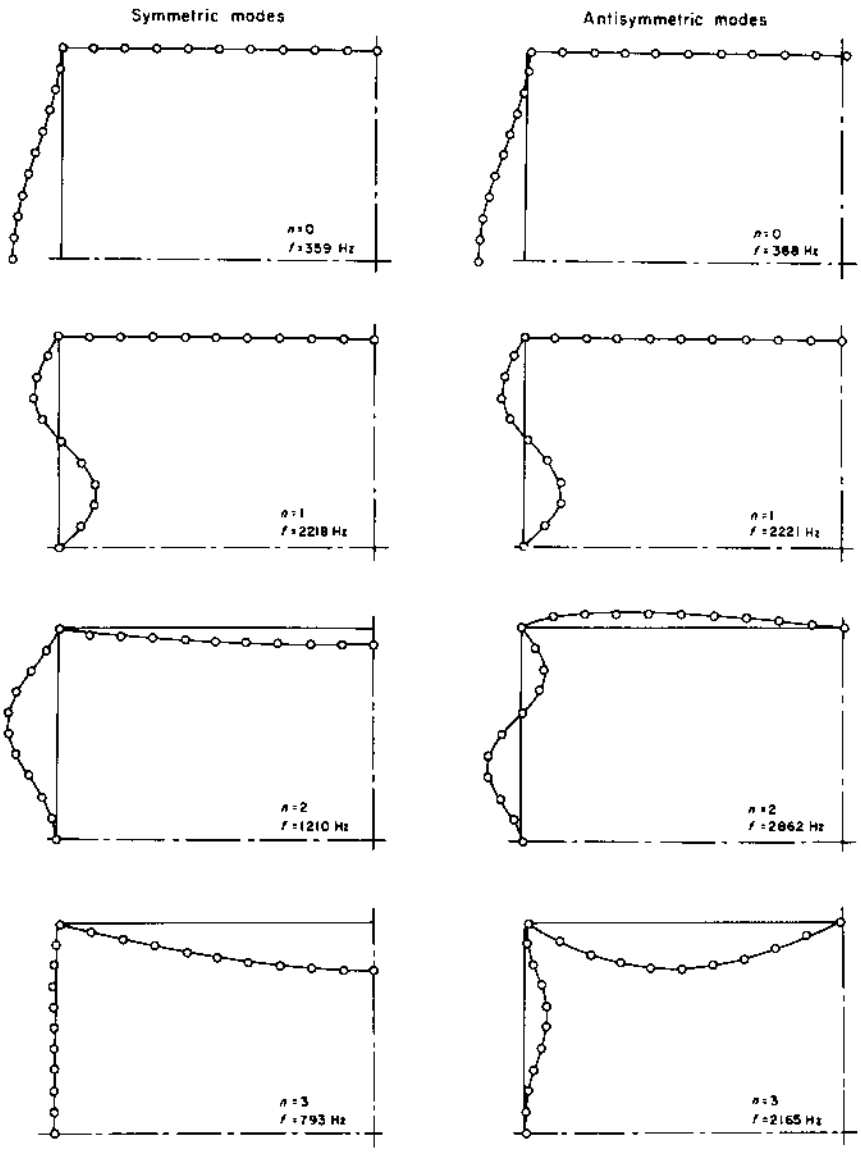

Figure 2. Various mode shapes of the hermetic can illustrated over one fourth of the can (the preservation of the 90° joint angle may be shown with a high resolution plot of the mode shapes).

between the end plates and the cylinder is observed for the higher values of N. This is also true for the higher modes occurring at the same value of n.

4. EXPERIMENTAL MODAL ANALYSIS

For the experimental modal analysis of the example case, two end plates were welded to a cylinder which itself had an axial welded seam. This hermetic can was laid on its side on soft foam with the welded axial seam on the bottom so that the measurement points would be kept away from the seam. The cylinder was excited with an impact hammer, but, since the end plates were lightly damped, they were excited with an electromechanical shaker fed with band limited Gaussian noise. Natural frequencies were

identified over the 0-2000 Hz frequency range. A survey of the measured accelerance spectra revealed that when both the driving and the driven (cross) points were located on either of the end plates, none of the frequencies matched those obtained when they both were located on the cylinder. This was interpreted to mean that the end plates and the cylinder were weakly coupled: in other words, the welded junctions did not hold the substructures together as rigidly as one would be inclined to assume in the theoretical model.

TABLE 2

Hermetic can: Comparison of predicted and measured natural frequencies (Hz)

n	Predictions		Measured	Dominating substructure
	SSM	FEM		
0	359	359	360	End plate
1	783	746	620	End plate
2	1210	1208	1200	Cylinder
3	793	793	750	Cylinder

In Table 2, some of the measured natural frequencies are compared with corresponding SSM predictions. As evident from Figure 2, except for the $n = 2$ mode, other frequencies of Table 2 represent modes for which either the end plate pair or the cylinder is the dominant vibrating substructure. This is why these modes were easily identifiable. For $n = 2$, the experimental results did not indicate any participation by the end plates even though the SSM results identified it to be a combination mode. Such discrepancies between the experiment and theory are mainly attributed to the flexibility of the welds and also to the warping of the end plates during the welding process which distorted the structure from its expected symmetry. Two decades ago, Faulkner [4] also found similar experimental problems associated with the warping of the end plates upon welding. Further research is required before our proposed method can handle such real life deviations.

George W. Woodruff
School of Mechanical Engineering,
Georgia Institute of Technology, Atlanta, Georgia 30332, *U.S.A.*

M. S. TAVAKOLI

Mechanical Engineering Department, Ohio State University,
206 *W.* 18*th Avenue, Columbus, Ohio* 43210, *U.S.A.*

R. SINGH

(*Received* 18 *April* 1989)

REFERENCES

1. M. S. TAVAKOLI and R. SINGH 1989 *Journal of Sound and Vibration* **130**, 97-123. Eigensolutions of joined/hermetic shell structures using the state space method.
2. M. S. TAVAKOLI and R. SINGH 1989 *American Society of Heating, Refrigeration and Air-Conditioning Engineers Transactions* **95**, 131-140. State space modeling of a refrigeration compressor shell dynamics.
3. M. S. TAVAKOLI 1987 *Ph.D. Thesis, The Ohio State University.* Dynamic synthesis of jointed/hermetic shell structures using the state space method.
4. L. L. FAULKNER 1969 *Ph.D. Thesis, Purdue University.* Vibration analysis of shell structures using receptances.

APPENDIX: NOMENCLATURE

$[C]$	substructure coupling matrix
D	bending stiffness, $= EH^3/12(1-\nu^2)$
E	Young's modulus of elasticity
M_x	bending moment resultant at x boundary
N_x	force resultant along x at x boundary
n	circumferential mode number
$S_{x\theta}$	in-plane Kirchhoff shear at x boundary
$[T(x_0, x)]$	transfer matrix between x_0 and x
V_x	transverse Kirchhoff shear at x boundary
W_1	axial displacement
W_2	circumferential displacement
W_3	transverse displacement
x	substructure co-ordinate spanning from boundary to boundary
x_{0i}, x_{1i}	initial and final boundary co-ordinates of substructure i
Z_i	co-ordinate normal to the surface of ith substructure
β_x	slope along x
ν	Poisson ratio
ρ	mass density
$\{\Phi(x)\}$	state vector at x boundary